Applicability of the localization-interaction model to magnetoconductivity studies of polyaniline films at the metal-insulator boundary

G. Tzamalis,* N. A. Zaidi, and A. P. Monkman
Department of Physics, University of Durham, South Road, Durham DH1 3LE, United Kingdom
(Received 20 February 2003; revised manuscript received 5 June 2003; published 9 December 2003)

Low temperature (down to 1.5 K) conductivity and high-field (up to 13.09×10^4 Oe) magnetoconductivity measurements were performed on three different polyaniline films doped with two dopant acids. The transport behavior of those systems, which lay on either side of the metal-insulator transition, was investigated within the framework of the localization-interaction model and parameters that can implicitly determine the degree of the disorder present in the systems have been evaluated. The suitability, consistency, and limitations of the model for the study of conducting polymers close to the metal-insulator transition are thoroughly discussed.

DOI: 10.1103/PhysRevB.68.245106 PACS number(s): 72.80.Le

I. INTRODUCTION

There were significant attempts in the early 1980s for the development of a theory that could describe the effects of Anderson localization[1–3] and the effects of electron-electron interactions[4–8] on the transport properties for disordered electronic systems. The scaling theory of localization[3] has lead to the localization-interaction model[9,10] that, as numerous studies from different groups have shown,[11–27] describes with considerable success the observed transport properties of homogeneously disordered metallic systems close to the metal-insulator (MI) transition.

Conducting polymers have exhibited that they can undergo a MI transition whose complex nature is primarily determined by the disorder, interchain interaction, and doping level, although the relative importance and precise contribution of those factors remains controversial.[28,29] One of the main issues of contention is whether disorder can be regarded as homogeneous or heterogeneous. In the case of homogeneous disorder, the three-dimensional localization-interaction model could be used for the study of transport phenomena in conducting polymers near the MI transition, whereas in the case of heterogeneous disorder it has been argued[30] that the system consists of crystalline domains embedded in amorphous (nonconducting) media and transport occurs by percolation of the charge carriers between the crystalline regions.[31] Recent advancements in the processibility of conducting polymers have significantly improved the quality of the materials by reducing the extent of the disorder in such a way that the localization length, which characterizes the extent of the electronic wave functions, becomes greater than the averaged-over structural coherence length that characterises the size of the crystalline regions.[18,32,33] In such a case the disorder can be regarded as homogeneous since the system sees an average of the random fluctuation of the disorder potentials and can, arguably, be described by the localization-interaction model.

One of the systems that has been shown to be suitable for investigation within the framework of the localization-interaction model is doped polyaniline (PANI). Following recent studies of its optical properties,[34–36] two different polyaniline systems have been used for low temperature (down to 1.5 K) conductivity and magnetoconductivity measurements: polyaniline doped with 10-camphorsulfonic acid (CSA) and polyaniline doped with 2-acrylamido-2-methyl-1-propanesulfonic acid (AMPSA). The variation of the doping level has provided samples with different degrees of disorder and consequently they lie on either side of the MI transition. The following study will comprehensibly examine the suitability and the limitations of the localization-interaction model for an implicit determination, through various parameters, of the degree of the disorder present in the polyaniline systems and their subsequent classification in the corresponding side of a disorder induced metal-insulator transition. Several issues regarding the applicability of the model will be clarified and more corroborating evidence regarding the intrinsic metallic character of PANI will be presented throughout comparative investigation of the differences between the distinct polyaniline systems. A comparison with the conclusions derived from the optical properties[34,35] will also be performed.

II. THEORETICAL FRAMEWORK

The localization-interaction model predicts behaviors different from those of periodic systems and provides quantum mechanical corrections to the semiclassical Boltzmann conductivity which arise in sufficiently disordered metals at low temperatures.[10] These corrections are the self-explanatory electron-electron interaction and the weak localization that tends to localize the electron wave function due to quantum interference. According to the localization-interaction model, the conductivity in the disordered metallic regime at low temperatures is given by[9]

$$\sigma(T)=\sigma(0)+m'T^{1/2}+BT^{p/2}, \tag{1}$$

where the second term arises from electron-electron interactions, while the last term is the correction to the zero-temperature conductivity due to localization effects.[21] The value of p is determined by the temperature dependence of the scattering rate, $\tau_{in}^{-1}\propto T^p$, of the dominant dephasing mechanism. Reported values of p range from $p=2.5$ to 3 for electron-phonon scattering, $p=2$ for inelastic electron-electron scattering (clean limit) or $p=3/2$ (dirty limit).[18] The

calculations by Belitz and Wysokinski[37] give $p=1$, close, to the metal-insulator transition. The parameter m' is given by the expression[4,21]

$$m' = a\left[\frac{4}{3} - \gamma\left(\frac{3F_\sigma}{2}\right)\right], \tag{2}$$

where $a \propto D^{-1/2}$ with D being the diffusion coefficient, γ is a parameter dependent on details of the electronic structure, and F_σ the interaction parameter, which is a complicated but monotonic function of the Thomas-Fermi screening wave vector K. It is related to the Fermi-liquid parameter F, which represents the screened electron-electron interactions averaged over the Fermi surface by the expression (Hartree interaction)[21]

$$F_\sigma = -\frac{32}{3F}[1 - 3F/4 - (1-F/2)^{3/2}], \tag{3}$$

where the Hartree factor F can be written as

$$F = (1/x)\ln(1+x), \tag{4}$$

with $x=(2k_F/K)^2$. The screening length K^{-1} becomes very large near the transition whereby F varies between 0 and 1, decreasing as the transition is approached. The parameter F_σ (always positive) follows the decrease of F, causing the parameter m' to change sign from negative to positive when $\gamma F_\sigma < 8/9$. Since $a \propto D^{-1/2}$ with D being the diffusion coefficient, $a \propto \sigma_0^{-1/2}$, and therefore a gives a contribution to m' in Eq. (2) that increases in magnitude as the metal-insulator transition is approached from the metallic to the insulating side. Deep in the metallic regime, m' is negative since F_σ is large, increasing as the transition is approached and changing sign when K^{-1} diverges at the metal-insulator transition.

In the framework of the localization-interaction model, the primary distinction between high and low magnetic field limits has different characteristic field limits for the interaction and the localization terms.[9] For the *e-e* interaction the distinction is made by comparing the Zeeman splitting energy of the electron (the energy quanta of a quantum-mechanical transition) $g\mu_B H$, where g is the electron gyromagnetic ratio (*g factor*) which is approximately equal to 2, to the thermal energy $k_B T$. Hence the *high*-field limit condition for the *e-e* interaction is $g\mu_B H \gg kT$ and after numerical substitution becomes $H/T \gg k_B/g\mu_B = 0.744\times 10^4$ Oe/K. In the case of the weak localization, the high-field condition is $H \gg (hc/2e) l_{in}^{-2}$, where l_{in} is the inelastic scattering length.

A. Electron-electron interactions

The quantum corrections to the magnetoconductance, due to *e-e* interactions, defined as

$$\Delta\sigma_I(H,T) = \sigma_I(H,T) - \sigma_I(0,T), \tag{5}$$

are given by the following expressions:[18,20]

$$\Delta\sigma_I(H,T) = -0.041 a (g\mu_B/k_B)^2 \gamma F_\sigma T^{-3/2} H^2 \quad \text{for } g\mu_B H \ll kT, \tag{6}$$

$$\Delta\sigma_I(H,T) = a\gamma F_\sigma T^{1/2} - 0.77 a (g\mu_B/k_B)^{1/2} \gamma F_\sigma H^{1/2} \quad \text{for } g\mu_B H \gg kT. \tag{7}$$

From the above equations it is apparent that the magnetoconductance due to *e-e* interactions is expected to behave as $H^{1/2}$ at very high and as H^2 at very low fields. Also the contribution of the *e-e* interactions to the magnetoconductance is always *negative*, arising from Zeeman splitting of the spin-up and spin-down bands.

An expression similar to Eq. (1) for the conductivity at low temperatures under the presence of a strong magnetic field, but due to *e-e* interactions only, can be easily obtained by combining the above equations

$$\sigma_I(H,T) = \sigma_I(H,0) + m_H T^{1/2} \tag{8}$$

where the coefficient m_H is given by

$$m_H = a\left[\frac{4}{3} - \gamma\left(\frac{F_\sigma}{2}\right)\right]. \tag{9}$$

The parameters present in Eq. (9) are identical to the ones of Eq. (2) since the equations were derived under the fundamental assumption that a, γ and F_σ are independent of the magnetic field. Since $\gamma F_\sigma = (m_H - m')/a$ and γF_σ is always positive, $m_H > m'$ with m_H having a positive range of values. As disorder increases, γF_σ decreases, causing m' to become positive when $\gamma F_\sigma < 8/9$. The application of a high magnetic field can, therefore, cause a change in the sign of the conductivity slope whenever $m' < 0$, namely in the samples for which $\gamma F_\sigma > 8/9$.

Values of m' and m_H, obtained from the magnetoconductance data, can characterize the extent of the disorder present in the sample and its relative position in an imaginary metal-insulator transition scale via the value of γF_σ, which, as mentioned above, decreases to zero as the sample goes from the metallic to the insulating side of the transition. Thus, from the magnetoconductance measurements parameters, unavailable from the conductivity data alone, that provide extra information about the sample properties can be deduced. Such procedure will be followed in the experimental section.

B. Weak localization

The primary distinction that must be made concerning the weak localization term is whether the spin-orbit effects are important or not. Studies[38–40] of disordered metallic films and doped semiconductors[20–22] where the spin-orbit coupling was strong have revealed a negative magnetoconductance. It appears that weak localization under the presence of strong spin-orbit effects changes to weak antilocalization due to destructive backscattering. Theoretical issues in the case of strong spin-orbits effects are yet to be decided. In conducting polymers, however, due to the dominance of atoms with relatively low atomic number, it should be expected the spin-orbit effects to be weak. This conjecture will, rather justifiably, be followed in the forthcoming analysis.

In the presence of weak spin-orbit effects, the magnetoconductance due to the weak localization term defined as

$$\Delta\sigma_L(H,T)=\sigma_L(H,T)-\sigma_L(0,T) \tag{10}$$

can be expressed by the following equations:[1,41,42]

$$\Delta\sigma_L(H,T)=(1/12\pi^2)(e/c\hbar)^2 G_0 l_{in}^3 H^2 \quad \text{for } H\ll(hc/2e)l_{in}^{-2}, \tag{11}$$

$$\Delta\sigma_L(H,T)=B_{WL}H^{1/2} \quad \text{for } H\gg(hc/2e)l_{in}^{-2}, \tag{12}$$

where $G_0=(e^2/\hbar)$ and B_{WL} is a constant with an estimated value for an isotropic material of the order of magnitude of $0.01\ \mathrm{S\,cm^{-1}\,Oe^{-1/2}}$ [11] and having a maximum value of $0.0435\ \mathrm{S\,cm^{-1}\,Oe^{-1/2}}$.[43] According to Eqs. (11) and (12), weak localization gives *positive* magnetoconductance. Therefore, the effect of the magnetic field is to suppress the localization effect. The high- and low-field behaviors of the magnetoconductance are identical to that due to *e-e* interactions, i.e., behavior proportional to $H^{1/2}$ at very high and to H^2 at very low fields.

C. Total corrections

The corrections to magnetoconductance (MC) due to *e-e* interactions and weak localization are additive, providing the following expression for the total magnetoconductance:

$$\Delta\sigma(H,T)=\sigma(H,T)-\sigma(0,T)=\Delta\sigma_1(H,T)+\Delta\sigma_L(H,T). \tag{13}$$

It has been surmised by various studies[20,41] that despite the importance of the interplay between those two interactions for the extent of the disorder present in the system, the *e-e* interactions are more dominant at lower temperatures and higher fields, while the weak localization effects are more dominant at higher temperatures and lower fields. The validity of such remarks will be explored during the analysis of the magnetoconductance data taken from PANI films.

III. EXPERIMENTAL PROCEDURE

A. Sample preparation

Using the emeraldine base form of PANi with high molecular weight ($M_w\sim 2\times10^5$ g/mol) as starting material, three different polyaniline systems were obtained by drop-casting from solution after homogenization: PANI-CSA films with 30% and 60% doping level among with PANI-AMPSA 50%.[44,45] Each doping level signifies a different molar ratio of dopant to the EB and the films, whose thickness ranged from 30-100 μm, obtained throughout this process were considered isotropic. The aging effect[46,47] in the conductivity of the samples was hardly noticeable ($\sim$2%); however, the preparation procedure does affect the random disorder present in the final system, but not to such a degree that inhibits any discussion considering distinctive physical tendencies in the samples.

B. Experimental setup

Conductivity and MC measurements were carried out in a helium cryostat with a superconducting magnet that enabled magnetic fields up to 13.09×10^4 Oe and temperatures ranging from room temperature to 1.5 K to be reached. The temperature was monitored with either Pt resistance thermometer (for $T>50$ K) or a carbon glass thermometer (for $T<50$ K).

The conductivity of the samples was measured using the ''four-in-line technique.'' The electrical contacts were made by placing four thin copper wires with conductive graphite adhesive onto the four gold strips that had been evaporated on the samples. The linear response in the current-voltage curve was confirmed and in order to avoid any additional sample heating, the dissipated power onto the sample did not exceed 1 μW. The magnetoconductance measurements were conducted with the magnetic field perpendicular to the film surface and, thus, to the current direction. The repeatability

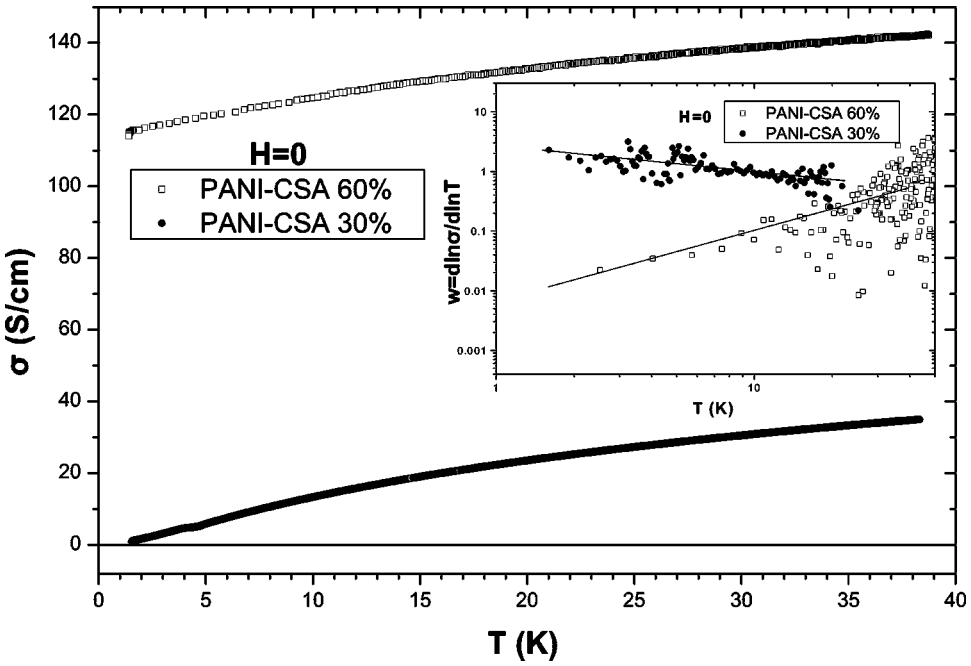

FIG. 1. The temperature dependence of the dc conductivity for PANI-CSA samples. The logarithmic plots of the activation energy W against temperature are shown in the inset. At low temperatures, ($T<20$ K), where the criterion is applicable, the PANI-CSA 60% film shows a positive slope (metallic regime), whereas the PANI-CSA 30% film shows a negative slope (insulating regime).

TABLE I. The reference conductivity values for the samples under investigation along with the fitting parameters of the localization-interaction model for a sample in the metallic regime of a MI transition. The MC percentage is calculated for $H=13.09\times10^4$ Oe and $T=1.5$ K. The relative errors of the fitting parameters are approximately 0.1%.

Sample	σ(295 K) (S/cm)	ρ_r	$\sigma_I(0)$ (S/cm)	m' $(\Omega\ \mathrm{m\ K^{1/2}})^{-1}$	$\sigma_I(H,0)$ (S/cm)	m_H $(\Omega\ \mathrm{cm\ K^{1/2}})^{-1}$	α	γF_σ	MC (%)
PANI-CSA 30%	52	57	-	-	-	-	-	-	−40
PANI-CSA 60%	120	1.06	108.63	3.88	94.40	8.86	8.51	0.59	−7
PANI-AMPSA 50%	100	1.22	66.04	11.51	63.55	13.86	11.28	0.21	0.7

of the results was confirmed by examining several samples from each category and small variations among samples of the same category can be attributed to different degrees of random disorder induced upon preparation.

IV. RESULTS AND DISCUSSION

A. Temperature dependence of conductivity

Low temperature ($T<10$ K) dependent conductivity measurements initially without an external magnetic field and, afterwards under a magnetic field $H=13.09\times10^4$ Oe were performed on PANI-CSA and PANI-AMPSA samples. The results from each sample category are presented separately for clarity purposes.

PANI-CSA films

According to a recent study,[34] PANI-CSA 60% and PANI-CSA 30% are, respectively, the most metallic and least metallic of all the PANI-CSA films studied thereby. Figure 1 shows the conductivity values as a function of temperature for those two samples. Their resistivity ratio is defined as $\rho_r=\sigma(295\ \mathrm{K})/\sigma(1.5\ \mathrm{K})$ and its values are included in Table I. From these values, it is surmised that PANI-CSA 60% is in the metallic regime ($\rho_r<2$), whereas PANI-CSA 30% is in the insulating regime ($10<\rho_r$) of a disorder induced metal-insulator transition.[48] Such classification is corroborated by the activation energy $W=d(\ln\sigma)/d(\ln T)$, shown in the inset of Fig. 1. Sample PANI-CSA 30% shows a negative temperature coefficient at low temperatures, while PANI-CSA 60% a positive one, indicating the former is on the insulating side of the MI transition whereas the latter is on the metallic. The activation energy criterion was applicable since the samples, as the conductivity plots of Fig. 1 testified, showed a negative temperature coefficient of resistivity at the low temperature regime. The agreement between the $W(T)$ plots and the resistivity ratio confirms the importance of these two factors for the precise identification of the metallic, critical and insulating regimes in conducting polymers.

Figure 2 shows the low temperature conductivity data of the PANI-CSA 60% sample with and without the presence of a strong magnetic field, $H=13.09\times10^4$ Oe. According to the localization-interaction, the conductivity of disordered system in the *metallic* regime is given by expression (1). At very low temperatures ($T<4$ K), the e-e interaction dominates over the weak-localization contribution to the conductivity[14,21,49] and the conductivity is given by

$$\sigma_I(T)=\sigma_I(0)+m'T^{1/2}, \tag{14}$$

while under the presence of a strong magnetic field ($H>8\times10^4$ Oe), the corresponding expression is

$$\sigma_I(H,T)=\sigma_I(H,0)+m_HT^{1/2}. \tag{15}$$

Equations (14) and (15) were successfully fitted to the PANI-CSA 60% low temperature conductivity data, as Fig. 2 dem-

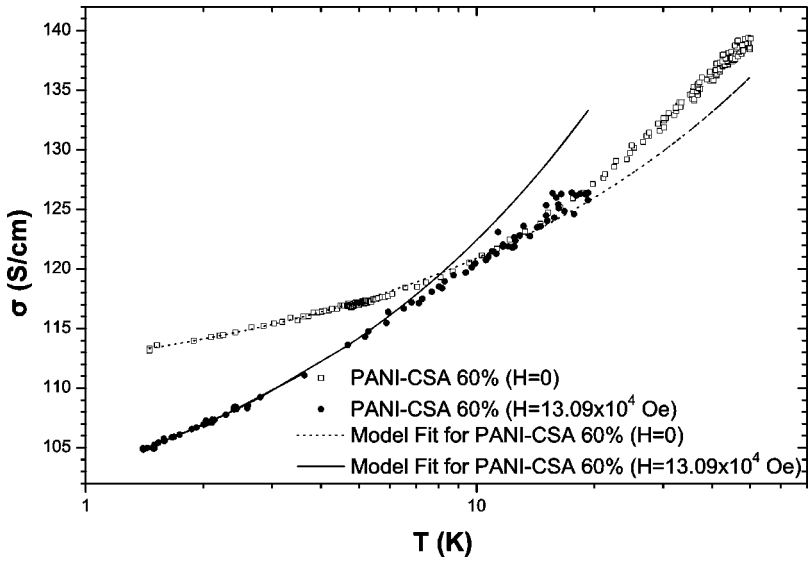

FIG. 2. Temperature dependence of the conductivity for the PANI-CSA 60% sample with and without the presence of an external magnetic field. Model fits were performed in the context of the localization-interaction model for samples in the metallic regime. The semilog plot illustrates clearly that the applicability of the model is limited at low temperatures.

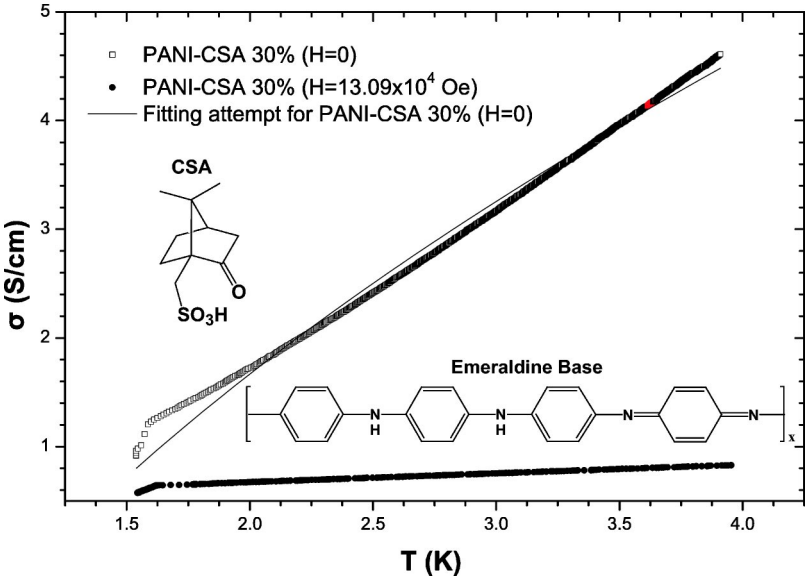

FIG. 3. Temperature dependence of the conductivity for the PANI-CSA 30% sample with and without the presence of an external magnetic field. Since the sample is in the insulating regime, attempts to fit, as in the case of the PANI-CSA 60% sample, the same model described by Eq. (14) have failed.

onstrates. Attempts to fit Eq. (1) to the data were abandoned due to problems of overparametrization. The values of the fitting parameters $\sigma_1(0)$, m', $\sigma_1(H,0)$ and m_H are summarized in Table I. Both samples showed negative magnetoconductance after the application of the magnetic field.

For a sample in the insulating regime, such as PANI-CSA 30%, Figure 3 demonstrates the unsuitability of the metallic regime expression for the low temperature conductivity. For samples in the insulating regime, the conductivity follows the activated temperature dependence of variable range hopping (VRH) among localized states below the mobility edge.[50,51] In this case, $\sigma(T)$ becomes exponential and is given by the general expression

$$\sigma(T)=\sigma_0 \exp\left[-\left(\frac{T_0}{T}\right)^x\right], \tag{16}$$

where σ_0 is a constant, $x=1/(1+d)$ (d the dimensionality of the system) and, for three-dimensional systems, $T_0=\text{const}/k_B N(E_F)L^3$ (L being the localization length). For three-dimensional hopping of noninteracting carriers $x=1/4$ (Mott's law), while in the Efros-Shklovskii limit,[52] where the interactions between localized electrons play an important role in the hopping transport, $x=1/2$. By substituting Eq. (16) into the expression for the activation energy $W=d(\ln\sigma)/d(\ln T)$, we find that

$$W=xT_0^x T^{-x} \tag{17}$$

or

$$\ln W=\ln(xT_0^x)-x\ln T. \tag{18}$$

The VRH parameters can, therefore, be determined from the slopes of the W versus T plots in the inset of Fig. 1. The values obtained for PANI-CSA 30% sample are $x=0.345$ and $T_0=60$ K, which are in the value range reported by other groups on similar (but not identical) systems.[33,53] The exponent x grows as the samples become more insulating and the charge transport becomes more characteristic of hopping on isolated chains with reduced dimensionality. In the current case, $d=1.9$ indicating a quasi-two-dimensional transport mechanism. It must be noted, however, that obtaining the VRH parameters from the $W(T)$ plots is not an entirely precise procedure since the $W(T)$ plots themselves are deduced by differentiating the measured conductivity data and it is well known in the field of numerical analysis that numerical differentiation is a high-risk technique that poses complicated problems, not always malleable, for an error-free application. The standard errors in the $W(T)$ plots can, therefore, become quite large (e.g., a relative error greater than 50%) depending on the differentiation technique used. However, since the plots have more of a comparative than absolute value, and considering the fact the same differentiation technique was used for every sample, we would expect the relative errors to be similar from sample to sample and that the general trends in the plots will remain distinguishable.

PANI-AMPSA 50% film

Figure 4 shows the low temperature conductivity data for the PANI-AMPSA 50% sample. It is observed that, contrary to PANI-CSA samples, the magnetoconductance increases after the application of a strong external magnetic field, $H=13.09\times10^4$ Oe. This observation will be discussed in detail in the magnetoconductance section that follows. The resistivity ratio and the slightly positive slope of the $W(T)$ curve indicate that the sample is on the metallic side, albeit closer to the transition that PANI-CSA 60%. Furthermore, the activation energy values of PANI-AMPSA film are greater than those of PANI-CSA 60% (metallic regime) and smaller than those of PANI-CSA 30% (insulating regime), suggesting that, since the reduced activation energy increases as the samples becomes more insulating, the film is at an intermediate position in an imaginary MI transition diagram. Following the same procedure with PANI-CSA 60%, the model curve fits are plotted in Fig. 5 and the fitting parameters are listed in Table I.

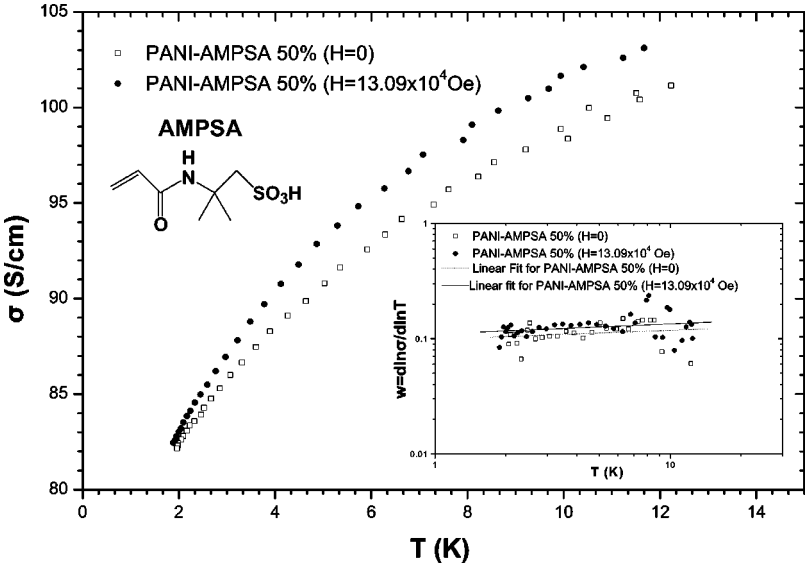

FIG. 4. The low temperature dependence of conductivity for the PANI-AMPSA 50% sample with and without the presence of an external magnetic field. The corresponding activation energy curves are logarithmically plotted in the inset.

Discussion

The results of all the samples studied are listed in Table I. According to the localization-interaction model, $m_H > m'$, something that is confirmed by the current results. As explained previously, the value of m' increases in magnitude as the MI transition is approached, viz. the more insulating samples have larger values of m'. This was found to be the case for the samples under investigation since the primary classification done by the resistivity ratio and the reduced activation energy plots is consistent with the values of m' that were derived by applying the localization-interaction model on the low temperature conductivity data.

From the values of m_H and m', the parameters a and γF_σ can be determined, after solving Eqs. (2) and (9), by the expressions

$$a = \frac{3}{8}(3m_H - m'), \tag{19}$$

$$\gamma F_\sigma = \frac{m_H - m'}{a}. \tag{20}$$

The values of a and γF_σ are listed in Table I. In accordance with the theory, a (γF_σ) increases (decreases) as the sample moves from the metallic to the insulating side of the MI transition. These values are similar to the ones found by other groups from studies on other conducting polymers close to the MI transition.[14,48,49] Since for both samples $\gamma F_\sigma < 8/9$, m' is positive showing that the samples are not deep in the metallic regime, where m' is negative, but rather they are close, on the metallic side, to the boundary of an MI transition. It is apparent that ρ_r, a and γF_σ, as Table I shows, along with m' can provide a consistent classification of a sample in respect to its degree of disorder and the position in a virtual MI transition diagram. This is achieved without any knowledge of the microscopic quantities that determine the charge transport such as carrier density, relaxation time, drawing a line between conducting polymers and inor-

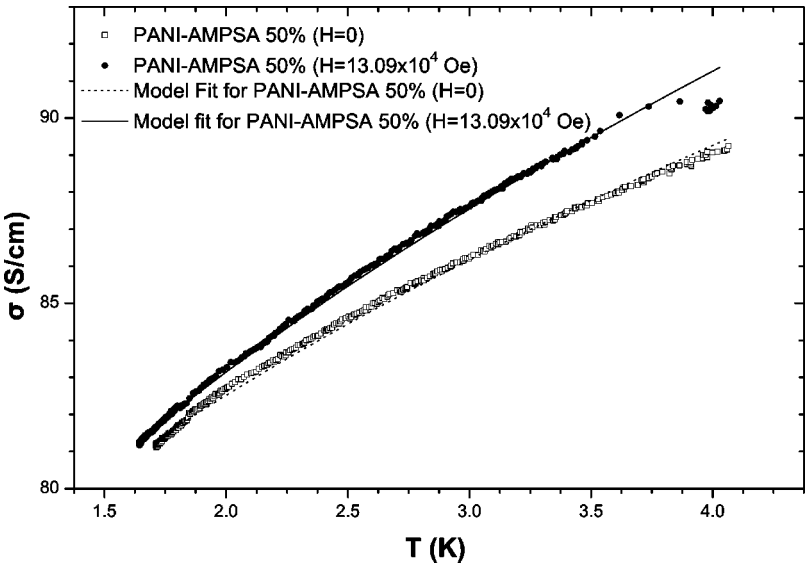

FIG. 5. The low temperature conductivity curves along with the localization-interaction model fits for the PANI-AMPSA 50% sample.

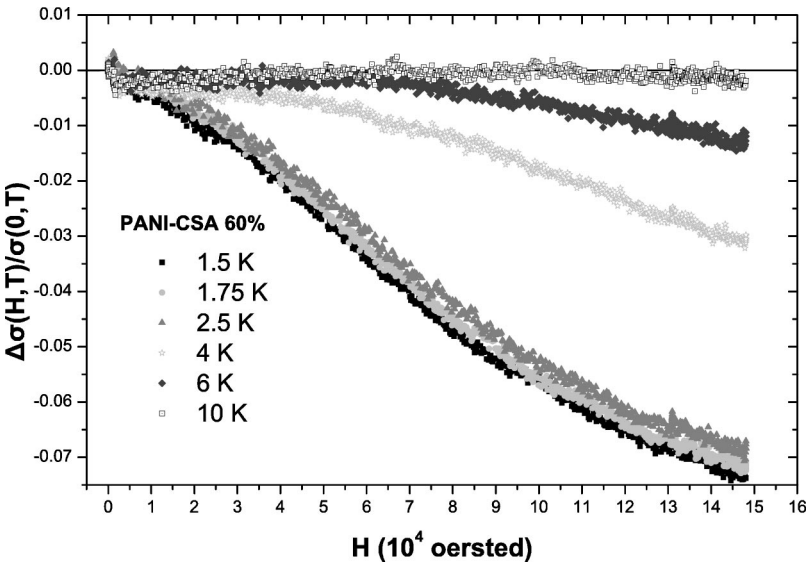

FIG. 6. Magnetoconductance as a function of the applied magnetic field for the PANI-CSA 60% at different temperatures.

ganic semiconductors[20–22] where such quantities are either known or can be precisely measured.

The classification of the samples according to a and γF_σ agrees with the results obtained using another order parameter, the product $k_F\lambda$ where k_F and λ are the Fermi wave vector and the mean free path respectively.[34] The values of $k_F\lambda$ were obtained within the framework of the localization-interaction model, but were derived from the optical properties of the samples, suggesting, thus, a considerable consistency in the sample's behavior.

Before proceeding with the magnetoconductance data, an important subtle point regarding the applicability of expressions (14) and (15) for the case of a sample in the metallic regime, but with *positive* magnetoconductance, must be made. According to the preceding theory, the above expressions were derived under the fundamental assumption that the low temperature conductivity is determined only by the e-e interaction. Since the e-e interaction leads always to negative magnetoconductance, the application of those expressions in the case of positive magnetoconductance, as in the case of the PANI-AMPSA 50% sample, seems, at first, questionable. However, in the case of a strong magnetic field $H=13.09\times10^4$ Oe, the inequality $H\gg(hc/2e)l_{in}^{-2}$ for $l_{in}>125$ Å is satisfied for the whole temperature range over which the fits were performed. It has been reported[54] that in the case of PANI-CSA samples $l_{in}\sim$150-300 Å for temperatures up to 5 K, and therefore the high field condition is assumed to be satisfied. This implies that the weak-localization contribution to the magnetoconductance is given by expression (12):

$$\Delta\sigma_L(H,T)=B_{WL}H^{1/2}. \tag{21}$$

According to Eq. (21), the weak-localization contribution to the conductivity at high fields and low temperatures is temperature independent (since B_{WL} is constant). Therefore for $H=13.09\times10^4$ Oe, $\Delta\sigma_L$ is constant and therefore can be incorporated in the constant $\sigma_I(H,0)$ of equation (15). Hence, the application of the localization-interaction model for a sample marginally in the metallic regime of a MI transition like PANI-AMPSA 50%, is formally justified.

B. Field dependency of magnetoconductance

Complementary information regarding the charge dynamics under a magnetic field can be obtained by measuring the magnetoconductance as a function of the applied field at different temperatures. This procedure has been followed on all the samples investigated in the previous section.

PANI-CSA 60%

Figure 6 shows the magnetoconductance of the sample under an applied magnetic field ranging from 0 to 14.8 $\times10^4$ Oe. The measurements were performed at various temperatures. The experimental values are similar to the ones reported by other studies on similar systems.[33,54] The maximum value of the MC is observed at $T=1.5$ K and is approximately 7.3%. The MC decreases with the increase of temperature and becomes almost negligible around 10 K. The decrease of the MC with increasing temperature can be attributed to the dominance of other scattering, both elastic and inelastic, mechanisms such as electron-phonon scattering that are temperature activated over the relatively weak localization and e-e interaction effects that constitute the sample's MC. The sample is not metallic enough (although it is in the metallic regime as discussed previously) to observe any considerably positive MC as in the case of weakly disordered metal.

The total change in conductivity is given in the high-field limit by the expression

$$\Delta\sigma(H,T)=a\gamma F_\sigma T^{1/2}-0.77a(g\mu_B/k_B)^{1/2}\gamma F_\sigma H^{1/2}+B_{WL}H^{1/2}. \tag{22}$$

Assuming once again that in the high magnetic field limit the weak localization contribution is small in comparison with the e-e interaction term and, thus, can be omitted, Eq. (22) can be approximated by

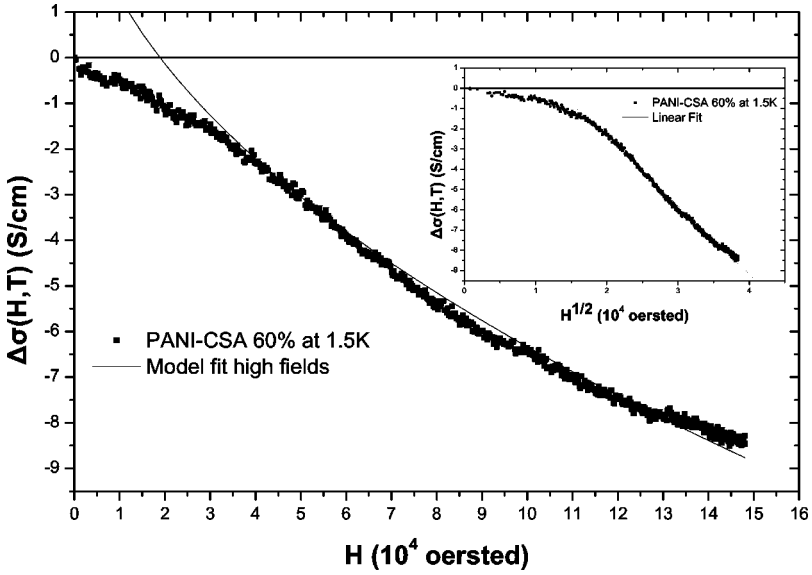

FIG. 7. The change in conductivity under a magnetic field of PANI-CSA 60% at 1.5 K and the high-field fit of the localization-interaction model given by Eq. (23). The inset plots $\Delta\sigma$ against $H^{1/2}$ to elucidate the suitability of Eq. (23) in the high-field region.

$$\Delta\sigma(H,T) = a\gamma F_\sigma T^{1/2} - 0.89 a\gamma F_\sigma H^{1/2}. \quad (23)$$

Equation (23) has been fitted to the MC data at different temperatures with $a\gamma F_\sigma$ as a fitting parameter giving similar results at each temperature. Figure 7 shows such a fit at 1.5 K. The value obtained for $a\gamma F_\sigma$ is 3.94 which is comparable with the values obtained in the previous section (Table I) which give that $a\gamma F_\sigma = 5.02$. The discrepancy can at first sight be attributed to the small influence of the weak localization (WL) in the measured curves and to other random errors that inhibit the accuracy of the fitting process. Another potential reason is that the parameter a as given by Eq. (19) may be temperature independent. Whether such case is valid here is a moot point, revealing that certain issues concerning the localization-interaction model remain unresolved. Nevertheless, the agreement is quite acceptable, suggesting an internal coherency in the model.

Ahlskog and co-workers[11,41] have tried calculating the e-e contribution without omitting the WL term of Eq. (22) since such omission is indeed valid only under approximation. After assuming that since the WL contribution B_{WL} is temperature independent, it can be cancelled out by subtracting the values of $\Delta\sigma$ at two different temperatures satisfying the high-field condition, they calculated the e-e coefficient $B_{EE} = -0.77 a (g\mu_B/k_B)^{1/2} \gamma F_\sigma H^{1/2}$ from the resulting values of $\Delta\sigma(H,T_1) - \Delta\sigma(H,T_2)$. However, they did not provide any further information regarding their calculation of B_{EE}. The aforementioned subtraction actually gives

$$\Delta\sigma(H,T_1) - \Delta\sigma(H,T_2) = a\gamma F_\sigma (T_1^{1/2} - T_2^{1/2}) + (B_{EE}^{T_1} - B_{EE}^{T_2}) H^{1/2}, \quad (24)$$

and by considering that the e-e interaction is temperature independent as well, the value of $a\gamma F_\sigma$ can be obtained. By trying different pairs of temperatures, a set of similar values of $a\gamma F_\sigma$ mostly greater than 5 was obtained, however such a method is sensitive to millikelvin temperature fluctuations leading, occasionally, to large dispersion when it is applied over a random set of temperature pairs. Hence, it should be applied with care. Nevertheless, the fact that the values of $a\gamma F_\sigma$ are greater than the value obtained from the $T^{1/2}$ dependence of $\sigma(T)$, demonstrates that in the first case the omission of the WL (positive contribution) does lead to an undervaluation of the absolute value of B_{EE}, or, in other words, to the underestimation of the contribution of the e-e interaction to the magnetoconductance. The above procedure provides us with further insight regarding recognition and quantification of the interplay of those two factors dominating the charge transport mechanism of a conducting polymer at low temperatures (low temperatures here refer to the temperature where the effect of other scattering processes to the charge transport in the material is negligible).

PANI-CSA 30%

The magnetic field dependence of the conductivity for sample PANI-CSA 30% at various temperatures is shown in Figure 8. The MC values displayed are significantly larger than the previous sample, exceeding 40% at 1.5 K. The dramatic increase of the negative MC as the sample crossed from the metallic (60% doping level) to the insulating regime (30%) is something typical for samples in the insulating regime of a MI transition.[12,32,48] The largely negative values of MC in the insulating regime can be attributed to the reduction of the overlap of the localized wave functions under the influence of the magnetic fields and the field's effect on the hopping transport among the localized states. The proportional relation among MC and the extent of disorder can be used in order to classify the systems according to their degree of disorder and their relative position on the insulating regime on a virtual MI transition diagram.

PANI-AMPSA 50%

Figure 9 plots the magnetoconductance of PANI-AMPSA 50% as a function of the magnetic field at different temperatures. The data are significantly different to the ones of the PANI-CSA samples, more resembling the magnetoconductance data of certain highly conducting polyacetylene

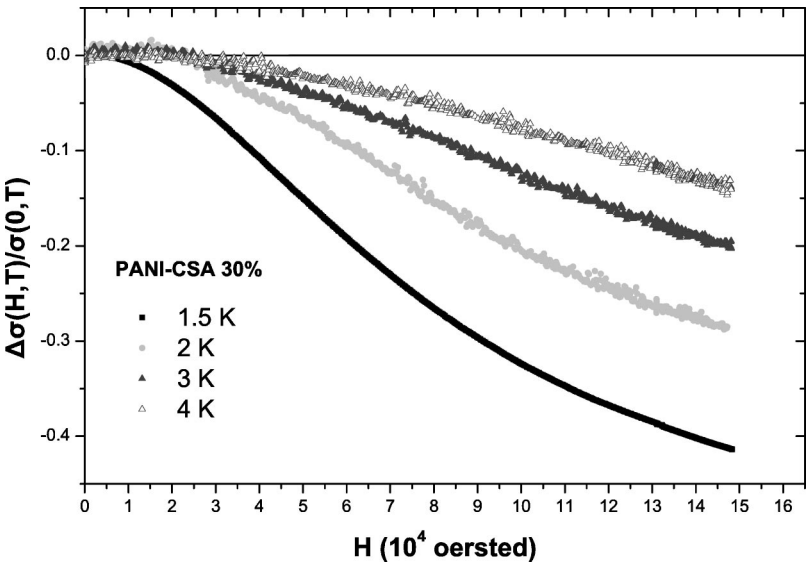

FIG. 8. Magnetoconductance as a function of the applied magnetic field for the PANI-CSA 30% at different temperatures.

samples as published by Nogami *et al.*,[43] but they lack the anisotropy and the high conductivity values of polyacetylene systems[55] and the difference between the MC properties of oriented and unoriented conducting polymers is usually significant. The positive contribution to the MC increases with increasing temperature and field. The existence of a local minimum for the MC curve at approximately 7.5×10^4 Oe for temperatures below 2 K cannot be explained in the context of the localization-interaction model for any choice of the parameters $a\gamma F_\sigma$ and B_{WL} of Eq. (22). At higher temperatures the MC becomes overwhelmingly positive and such rapid switch from negative to positive MC cannot be explained with the assumption that $a\gamma F_\sigma$ and B_{WL} are temperature and field independent since it is obvious that such increase requires modification of the coefficients in each of the three terms of Eq. (22). Hence, the three-dimensional localization theory is not suitable for interpreting the present case.

The inadequacy of the localization-interaction model is not, however, terminal. One of its main theoretical assumptions was that it is valid only for samples in the metallic regime and it is by no means clear that the theory is applicable very near to the transition (always on the metallic regime). The sample PANI-AMPSA 50% was found to be, from the activation energy plots and its resistivity ratio value, in the metallic regime, but closer to the transition in comparison to PANI-CSA 60% where the application of the model was found to be successful, as the values of Table I testify. Another factor that could explain such an insufficiency is the fact that, as Fig. 9 shows, the maximum MC measured is approximately 1.8%, a value that is strikingly smaller than almost any reported value for conjugated polymers.[49,54] Such small changes in the conductivity could be affected or even induced by the temperature fluctuations of the sample which are of the order of a tenth of a Kelvin. A quick look at the plots of Fig. 9 reveals a greater degree of dispersion than other samples. However, such a dispersion cannot be an excuse for an altogether dismissal of the current plots since the existence of a certain tendency is traceable enough to be attributed to random factors occurred during

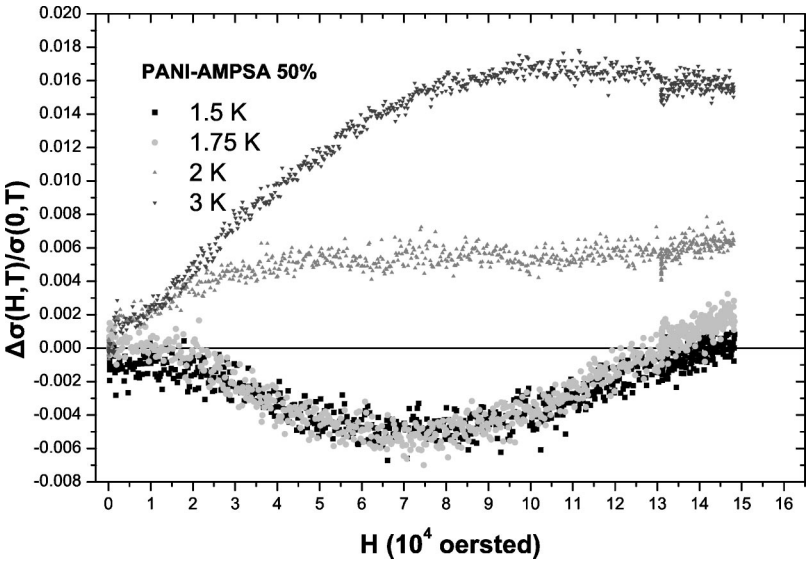

FIG. 9. Magnetoconductance as a function of the applied magnetic field for the PANI-AMPSA 50% at different temperatures.

the measurement session. The only safe conclusion that can currently be made is that the magneto-transport properties of the PANI-AMPSA 50% cannot be entirely understood within the present theoretical context since from the shape of the plots either $a\gamma F_{\sigma}$ or B_{WL} are not constant but H dependent or a new term/process is required.

V. SUMMARY

Low temperature magnetoconductance measurements were performed on three different polyaniline systems. The low temperature conductivity measurements enabled a primary classification of the materials in respect to the extent of the disorder present in their system that determined their position on a virtual metal-insulator transition diagram. More rigid evidence was provided by studying the effect of a varying magnetic field on the charge transport and attempting to interpret it in the context of the 3D localization-interaction model which is valid for samples in the disordered metallic regime of the MI transition. The model, despite certain shortcomings, can consistently interpret the charge transport properties of a sample being on the metallic side of the transition. An estimate of the competitive contribution of the e-e interaction and weak-localization was obtained. However, the model is found to be inadequate for samples on the metallic side but close to the transition, whereas in the insulating regime the charge transport occurs through variable-range hopping among localized states. The importance of MC measurements for a sensitive investigation of the microscopic charge transport mechanism in conducting polymers remains undisputed, although there are still unresolved theoretical issues, prompting the need for an improvement of the available models such as investigating any potential field or temperature dependency of the constants involved in the model.

ACKNOWLEDGMENTS

We are highly indebted to Dr. Stephen Blundell and Chris Steer for their permission and help in using the equipment of Clarendon Laboratory, Oxford, where the measurements were performed.

*Present address: Institute for Physical, Nuclear and Macromolecular Chemistry and Material Science, Philipps-University of Marburg, Hans Meerwein Strasse, D-35032 Marburg, Germany. Email address: georgios.tzamalis@dunelm.org.uk

[1] A. Kawabata, Solid State Commun. **34**, 431 (1980).
[2] A. Kawabata, J. Phys. Soc. Jpn. **50**, 2461 (1981).
[3] E. Abrahams, P. W. Anderson, D. C. Licciardello, and T. V. Ramakrishnan, Phys. Rev. Lett. **42**, 673 (1979).
[4] B. L. Altshuler and A. G. Aronov, Solid State Commun. **46**, 429 (1983).
[5] B. L. Altshuler, A. G. Aronov, and D. E. Khmelnitskii, Pis'ma Zh. Eksp. Teor. Fiz. **36**, 157 (1982) [JETP Lett. **36**, 195 (1982)].
[6] B. L. Altshuler and A. G. Aronov, Pis'ma Zh. Eksp. Teor. Fiz. **33**, 515 (1981) [JETP Lett. **33**, 499 (1981)].
[7] B. L. Altshuler, A. G. Aronov, and A. Y. Zuzin, Solid State Commun. **44**, 137 (1982).
[8] A. L. Efros and M. Pollak, *Electron-Electron Interactions in Disordered Systems* (North-Holland, New York, 1985).
[9] P. A. Lee and T. V. Ramakrishnan, Rev. Mod. Phys. **57**, 287 (1985).
[10] D. Belitz and T. R. Kirkpatrick, Rev. Mod. Phys. **66**, 261 (1994).
[11] M. Ahlskog and M. Reghu, J. Phys.: Condens. Matter **10**, 833 (1998).
[12] M. Ahlskog, R. Menon, A. J. Heeger, T. Noguchi, and T. Ohnishi, Phys. Rev. B **55**, 6777 (1997).
[13] M. Ahlskog, M. Reghu, and A. J. Heeger, J. Phys.: Condens. Matter **9**, 4145 (1997).
[14] A. Aleshin, R. Kiebooms, R. Menon, F. Wudl, and A. J. Heeger, Phys. Rev. B **56**, 3659 (1997).
[15] A. N. Aleshin, N. B. Mironkov, A. V. Suvorov, J. A. Conklin, T. M. Su, and R. B. Kaner, Phys. Rev. B **54**, 11638 (1996).
[16] A. N. Aleshin, N. B. Mironkov, A. V. Suvorov, I. O. Usov, J. A. Conklin, T. M. Su, and R. B. Kaner, J. Phys.: Condens. Matter **10**, 4867 (1998).
[17] M. Reghu, K. Vakiparta, Y. Cao, and D. Moses, Phys. Rev. B **49**, 16162 (1994).
[18] R. Menon, in *Handbook of Organic Conductive Molecules and Polymers*, edited by H. S. Nalwa (Wiley, Chichester, 1997), Vol. 4, p. 4v.
[19] C. O. Yoon, M. Reghu, D. Moses, and A. J. Heeger, Phys. Rev. B **49**, 10851 (1994).
[20] P. Dai, Y. Z. Zhang, and M. P. Sarachik, Phys. Rev. B **46**, 6724 (1992).
[21] P. H. Dai, Y. Z. Zhang, and M. P. Sarachik, Phys. Rev. B **45**, 3984 (1992).
[22] S. Bogdanovich, P. H. Dai, M. P. Sarachik, and V. Dobrosavljevic, Phys. Rev. Lett. **74**, 2543 (1995).
[23] E. Abrahams, S. V. Kravchenko, and M. P. Sarachik, Rev. Mod. Phys. **73**, 251 (2001).
[24] C. Segal, A. Gladkikh, M. Pilosof, H. Behar, M. Witcomb, and R. Rosenbaum, J. Phys.: Condens. Matter **10**, 123 (1998).
[25] R. Rosenbaum, P. Haberkern, P. Haussler, E. Palm, T. Murphy, S. Hannahs, and B. Brandt, J. Phys.: Condens. Matter **12**, 9735 (2000).
[26] R. Rosenbaum, A. Milner, R. Haberkern, P. Haussler, E. Palm, T. Murphy, S. Hannahs, and B. Brandt, J. Phys.: Condens. Matter **13**, 3169 (2001).
[27] R. Rosenbaum, A. Heines, M. Karpovski, M. Pilosof, and M. Witcomb, J. Phys.: Condens. Matter **9**, 5413 (1997).
[28] A. J. Heeger, J. Phys. Chem. B **105**, 8475 (2001).
[29] V. N. Prigodin and A. J. Epstein, Synth. Met. **125**, 43 (2001).
[30] A. B. Kaiser, Adv. Mater. (Weinheim, Ger.) **13**, 927 (2001).
[31] A. J. Epstein, J. Joo, R. S. Kohlman, G. Du, A. G. Macdiarmid, E. J. Oh, Y. Min, J. Tsukamoto, H. Kaneko, and J. P. Pouget, Synth. Met. **65**, 149 (1994).
[32] R. Kiebooms, R. Menon, and K. Lee, in *Handbook of Advanced Electronic and Photonic Materials and Devices*, edited by H. S. Nalwa (Academic Press, San Diego, CA, 2001), Vol. 8, p. 10v.
[33] R. S. Kohlman and A. J. Epstein, in *Handbook of Conducting Polymers*, edited by T. A. Skotheim, R. L. Elsenbaumer and J. R. Reynolds (Dekker, New York, 1998).
[34] G. Tzamalis, N. A. Zaidi, C. C. Homes, and A. P. Monkman,

Phys. Rev. B **66**, 085202 (2002).
[35] G. Tzamalis, N. A. Zaidi, C. C. Homes, and A. P. Monkman, J. Phys.: Condens. Matter **13**, 6297 (2001).
[36] G. Tzamalis, N. A. Zaidi, C. C. Homes, and A. P. Monkman, Synth. Met. **135–136**, 369 (2003).
[37] D. Belitz and K. I. Wysokinski, Phys. Rev. B **36**, 9333 (1987).
[38] G. Bergmann, Phys. Rev. B **28**, 2914 (1983).
[39] G. Bergmann, Phys. Rev. Lett. **48**, 1046 (1982).
[40] G. Bergmann, Phys. Rev. B **25**, 2937 (1982).
[41] M. Ahlskog, M. Reghu, A. J. Heeger, T. Noguchi, and T. Ohnishi, Phys. Rev. B **53**, 15529 (1996).
[42] M. Ahlskog and R. Menon, J. Phys.: Condens. Matter **10**, 7171 (1998).
[43] Y. Nogami, H. Kaneko, H. Ito, T. Ishiguro, T. Sasaki, N. Toyota, A. Takahashi, and J. Tsukamoto, Phys. Rev. B **43**, 11829 (1991).
[44] P. N. Adams, P. J. Laughlin, and A. P. Monkman, Synth. Met. **76**, 157 (1996).
[45] P. N. Adams, P. J. Laughlin, A. P. Monkman, and A. M. Kenwright, Polymer **37**, 3411 (1996).
[46] P. Rannou, M. Nechtschein, J. P. Travers, D. Berner, A. Wolter, and D. Djurado, Synth. Met. **101**, 734 (1999).
[47] P. Rannou, A. Wolter, J. P. Travers, B. Gilles, and D. Djurado, J. Chim. Phys. Phys.-Chim. Biol. **95**, 1396 (1998).
[48] R. Menon, C. O. Yoon, D. Moses, A. J. Heeger, and Y. Cao, Phys. Rev. B **48**, 17685 (1993).
[49] A. Aleshin, R. Kiebooms, R. Menon, and A. J. Heeger, Synth. Met. **90**, 61 (1997).
[50] N. F. Mott, *Conduction in Non-Crystalline Materials* (Oxford University Press, Oxford, 1987).
[51] N. F. Mott and E. A. Davis, *Electronic Processes in Non-Crystalline Materials* (Clarendon Press, Oxford, 1979).
[52] B. I. Shklovskii and A. L. Efros, *Electronic Properties of Doped Semiconductors* (Springer-Verlag, Berlin, 1984).
[53] M. Reghu, Y. Cao, D. Moses, and A. J. Heeger, Phys. Rev. B **47**, 1758 (1993).
[54] R. Menon, C. O. Yoon, D. Moses, and A. J. Heeger, in *Handbook of Conducting Polymers* (Ref. 33).
[55] A. N. Aleshin, V. I. Kozub, D. S. Suh, and Y. W. Park, Phys. Rev. B **64**, 224208 (2001).